

Pemphigus Vulgaris IgG-induced Desmoglein-3 Endocytosis and Desmosomal Disassembly Are Mediated by a Clathrin- and Dynamin-independent Mechanism^{*[5]}

Received for publication, December 10, 2007, and in revised form, April 18, 2008. Published, JBC Papers in Press, April 23, 2008, DOI 10.1074/jbc.M710046200

Emmanuella Delva^{†§}, Jean Marie Jennings[§], Catharine C. Calkins^{§¶}, Margaret D. Kottke[¶], Victor Faundez[§], and Andrew P. Kowalczyk^{§¶1}

From the [†]Graduate Program in Biochemistry, Cell, and Developmental Biology, [§]Department of Cell Biology, and [¶]Department of Dermatology, Emory University, Atlanta, Georgia 30332

Pemphigus vulgaris (PV) is a life-threatening autoimmune disease characterized by oral mucosal erosions and epidermal blistering. The autoantibodies generated target the desmosomal cadherin desmoglein-3 (Dsg3). Previous studies demonstrate that upon PV IgG binding, Dsg3 is internalized and enters an endo-lysosomal pathway where it is degraded. To define the endocytic machinery involved in PV IgG-induced Dsg3 internalization, human keratinocytes were incubated with PV IgG, and various tools were used to perturb distinct endocytic pathways. The PV IgG-Dsg3 complex failed to colocalize with clathrin, and inhibitors of clathrin- and dynamin-dependent pathways had little or no effect on Dsg3 internalization. In contrast, cholesterol binding agents such as filipin and nystatin and the tyrosine kinase inhibitor genistein dramatically inhibited Dsg3 internalization. Furthermore, the Dsg3 cytoplasmic tail specified sensitivity to these inhibitors. Moreover, inhibition of Dsg3 endocytosis with genistein prevented disruption of desmosomes and loss of adhesion in the presence of PV IgG. Altogether, these results suggest that PV IgG-induced Dsg3 internalization is mediated through a clathrin- and dynamin-independent pathway and that Dsg3 endocytosis is tightly coupled to the pathogenic activity of PV IgG.

Desmosomes are adhesive junctions that provide robust adhesion between epithelial cells (1, 2). These organelles are prominent in tissues that experience substantial mechanical stress such as the heart, bladder, gastrointestinal mucosa, and skin. Desmosomes are comprised primarily of proteins from three major families, the desmosomal cadherins desmogleins and desmocollins, armadillo proteins such as plakoglobin and the plakophilins, and members of the plakin family of cytolinkers such as desmoplakin (1–3). Together, these proteins contribute to tissue integrity by coupling adhesive interactions

mediated by the desmosomal cadherins to the keratin intermediate filament cytoskeleton, thereby integrating adhesive and cytoskeletal networks throughout the cells in a tissue. Although critical for tissue integrity, desmosomes are often remodeled and contribute to dynamic processes during development and wound healing. Furthermore, desmosomal components may also play pivotal roles in keratinocyte differentiation, morphogenesis, and tissue patterning as well as epithelial-mesenchymal transitions (4, 5).

Pemphigus vulgaris (PV)² is a potentially fatal autoimmune skin disease in which autoantibodies are generated against the desmosomal cadherin, desmoglein-3 (Dsg3) (6–8). Dsg3, a 130-kDa glycoprotein, is found primarily in the spinous and basal layers of the epidermis and throughout the oral mucosa (9). As a result, PV is characterized histologically by suprabasal loss of cell-cell adhesion (acantholysis) and clinically by blistering of the skin and erosion of mucous membranes (7, 8). A wide range of approaches have demonstrated that Dsg3 is the key target of PV IgG (10, 11). In addition, experimentally generated mice in which the Dsg3 gene has been ablated exhibit histopathological characteristics of PV patients (12). However, the precise cellular mechanism by which acantholysis occurs in response to PV IgG remains controversial.

The epitopes on Dsg3 that are recognized by PV patient IgG and pathogenic monoclonal Dsg3 antibodies have been mapped and reside predominantly in the amino-terminal domain of Dsg3, a region of cadherins that structural studies have implicated in forming the adhesive interface (13–17). These types of studies argue strongly that PV IgG may cause loss of adhesion by steric hindrance of Dsg3 ectodomain interactions (7). However, other studies suggest that keratinocyte responses are needed for cells to lose adhesion (18). For example, desmosomes remain intact and keratinocytes remain adherent when incubated in the presence of PV IgG at 4 °C even though PV IgG are bound to Dsg3 (19). In fact, keratinocytes must be incubated at 37 °C for several hours to detect substantial loss of adhesive strength. These and other data favor the hypothesis that keratinocyte responses are required for the loss of adhesion caused by PV IgG. These responses may include alterations in p38 mitogen-activated protein kinase (MAPK)

^{*} This work was supported, in whole or in part, by National Institutes of Health Grants R01 AR048266, R01 AR050501, R21AR50779 (to A. P. K.), F31 CA110278-02 (to E. D.), and T32 AR007587 (to M. D. K.). The costs of publication of this article were defrayed in part by the payment of page charges. This article must therefore be hereby marked “advertisement” in accordance with 18 U.S.C. Section 1734 solely to indicate this fact.

^[5] The on-line version of this article (available at <http://www.jbc.org>) contains supplemental Movies 1 and 2.

¹ To whom correspondence should be addressed: Dept. of Cell Biology, 615 Michael St., Rm. 465, Atlanta, GA 30322. Tel.: 404-727-8517; Fax: 404-727-6256; E-mail: akowalc@emory.edu.

² The abbreviations used are: PV, pemphigus vulgaris; Dsg3, desmoglein-3; Dyn, dynamin; CTB, cholera toxin subunit B; EGF, epidermal growth factor; IL-2R, interleukin-2 receptor; NHK, normal human keratinocyte; VE, vascular endothelial.

Mechanism of Pemphigus Vulgaris IgG-induced Dsg3 Endocytosis

pathways (20), Rho GTPase activity (21), activation of c-Myc through plakoglobin-mediated signaling mechanisms (22), and other cellular responses that influence cell-cell adhesive interactions (23, 24).

Early studies demonstrated that PV IgG are internalized and targeted to lysosomes, and investigators postulated that PV IgG endocytosis might be coupled to the loss of adhesion characteristic of this disease (25, 26). In fact, several studies indicate that Dsg3 internalization and destabilization of desmosome integrity may be a key keratinocyte response to PV IgG. For example, PV IgG disrupts the assembly of functional desmosomes and causes rapid internalization and degradation of Dsg3 (5, 19, 27). Clathrin-dependent and clathrin-independent pathways represent the two major routes for internalization of cell surface receptors (28–30). Clathrin-mediated endocytosis, the most thoroughly studied endocytic pathway, is characterized by the formation of clathrin-coated pits at the plasma membrane. Clathrin-dependent endocytosis requires the GTPase dynamin (31–33), which participates in the budding of clathrin-coated vesicles that are then destined for endosomal compartments. Clathrin-independent endocytosis, on the other hand, is less well understood. However, many endocytic pathways fall under this category and include caveolae-mediated endocytosis and micro and macropinocytosis as well as pathways that are both clathrin- and caveolae-independent (30). Defining how specific receptors are internalized from the plasma membrane is critical for understanding how cells control the presentation of the receptor on the cell surface.

In the current study a series of approaches was used to selectively manipulate various endocytic pathways and thereby reveal the mechanism of PV IgG-induced-Dsg3 internalization. The results indicate that the Dsg3 cytoplasmic tail mediates Dsg3 internalization in response to PV IgG through a clathrin- and dynamin-independent endocytic pathway. Furthermore, in cells treated with PV patient IgG, inhibition of Dsg3 endocytosis prevents Dsg3 down-regulation, desmoplakin mislocalization, and loss of adhesion in functional assays. These findings provide evidence that destabilization of Dsg3 through clathrin-independent endocytic pathways is functionally coupled to the loss of keratinocyte adhesion strength in response to PV IgG.

EXPERIMENTAL PROCEDURES

Cells and Culture Conditions—Normal human keratinocytes (NHKs) were isolated and cultured as described previously (19). Briefly, NHKs were isolated from neonatal foreskin and cultured in keratinocyte growth medium (Cambrex Corp., East Rutherford, NJ). NHKs were used for experimentation at passage 2 or 3. For experiments, cells were shifted to media containing 0.5 mM calcium 16–18 h before treatments and remained in this medium throughout the duration of the experiments.

Antibodies and Ligands—Alexa Fluor EGF-488 and cholera toxin B (CTB)-488 were obtained from Invitrogen. The CD59 fluorescein isothiocyanate-conjugate monoclonal antibody was purchased from Millipore (Billerica, MA). The monoclonal clathrin antibody was purchased from BD Transduction Laboratories. Monoclonal IL-2 receptor (IL-2R) was obtained from R&D Systems. Appropriate species cross-absorbed secondary

antibodies conjugated to various Alexa Fluors (Molecular Probes, Eugene, OR) were used for dual-label immunofluorescence. Normal human serum was obtained from Irvine Scientific (Santa Ana, CA). PV IgG was a kind gift from Dr. Robert Swerlick (Emory University, Atlanta, GA) and Dr. Masayuki Amagai (Keio University School of Medicine, Tokyo) (8). Monoclonal anti-Dsg3 antibodies AK15 and AK23 (17) were kind gifts from Dr. Masayuki Amagai.

Adenoviruses—A chimeric protein comprising the IL-2R extracellular domain and the VE-cadherin cytoplasmic tail was generated as described previously (34). A construct encoding the extracellular domain of the IL-2R (35) was used to construct a chimeric cDNA with the IL-2R extracellular domain, the entire Dsg3 cytoplasmic tail, and a carboxyl-terminal FLAG epitope tag. The Dsg3 cytoplasmic domain construct was generated by PCR using the following primers: 5-primer, 5'-GCCATGACTAGTAGTGTGACTGTGGGGCAGGTTCTACT; 3-primer, 5'-CCGGATATCCTACTTATCGTCGTCATCCTTGTAATCTATTAGACGGGAGCAAGGATCCTCTGTACA. The 3-primer includes an in-frame FLAG epitope tag followed by a stop codon. The resulting PCR product was ligated into pKS followed by subcloning into the pAD-Track-CMV vector. All constructs were characterized fully by DNA sequence analysis, Western blot, and immunofluorescence analysis. Adenoviruses carrying the IL-2R-Dsg3_{cyto}-FLAG chimeric construct were produced using the pAdeasy adenovirus-packaging system as described previously (34, 36). Hemagglutinin (HA)-dyn2WT and HA-dyn2K44A were kind gifts from Dr. Sandra Schmid (The Scripps Institute, La Jolla). The caveolin-1 Y14F virus was a kind gift from Dr. Masuko Ushio-Fukai (University of Illinois at Chicago).

Immunofluorescence—NHKs were prepared for immunofluorescence as described previously (19). Briefly, cells were cultured on glass coverslips and shifted to media containing 0.5 mM calcium 16–18 h before treatment. Under the culture conditions used throughout this study, the keratinocytes predominantly expressed Dsg3 and low but detectable levels of Dsg1. For most experiments keratinocytes were incubated with affinity-purified human or mouse PV IgG on ice for 30 min to 1 h at a concentration of up to 1 mg/ml (diluted in media containing 0.5 mM calcium) to label the cell surface. Both human and mouse IgG were left on the cells throughout the duration of the experiment. Cells were then transferred to 37 °C for the indicated internalization times. After incubation at 37 °C, cells were returned on ice and treated with acid wash solution (3% bovine serum albumin, 25 mM glycine, pH 2.7) to remove cell surface-bound antibody. Cells were then fixed on ice using either –20 °C methanol for 5 min or 3.7% paraformaldehyde (Electron Microscopy Sciences, Hatfield, PA) for 10 min followed by extraction in 0.5% Triton X-100 (Roche Diagnostics) for 7 min. To detect cell surface levels of Dsg3, cells were fixed on ice for 10 min in 3.7% paraformaldehyde. After paraformaldehyde fixation, monoclonal anti-Dsg3 antibody AK15 (17) was used to stain for cell surface Dsg3. A Leica DMR-E fluorescence microscope equipped with narrow band-pass filters and a Hamamatsu Orca camera was used for image acquisition.

TABLE 1
Requirements necessary for internalization via distinct endocytic pathways

Endocytic pathway	Clathrin-mediated	Caveolae-mediated	Non-caveolar raft-dependent
Dependent on clathrin	×		
Dependent on caveolin		×	
Sensitive to hypertonic sucrose, K ⁺ depletion, and chlorpromazine	×		
Sensitive to cholesterol-perturbing agents <i>i.e.</i> filipin and nystatin		×	×
Dependent on dynamin activity	×	×	
Dependent on tyrosine kinase activity	×	×	×

Images were captured and processed using Simple PCI (Compix, Inc., Cranberry Township, PA).

Manipulation of Endocytic Pathways—IgG internalization was performed as previously described (19). NHKs were pretreated with 5 μ M filipin III (Sigma), 40 mM genistein (Sigma), 10 μ M nystatin (Sigma), 10 μ g/ml chlorpromazine (Sigma), and hypertonic sucrose (0.4 M sucrose) for 1 h at 37 °C. For K⁺ depletion, cells were first incubated in hypotonic media (50% K⁺ depletion solution, 50% H₂O) for 5 min at 37 °C followed by incubation in K⁺ depletion solution (20 mM Hepes, 140 mM NaCl, 1 mM CaCl₂, 1 mM MgCl₂, pH 7.4) for 30 min at 37 °C. Cells were then incubated with a pathogenic mouse monoclonal antibody against the extracellular domain of Dsg3, AK23 (17) (diluted in media containing 0.5 mM calcium) on ice for 30 min. Cells were then washed 3 times with PBS⁺ (Mediatech, Manassas, VA) (or K⁺ depletion solution) followed by incubation at 37 °C for various times in media containing 0.5 mM calcium. After incubation at 37 °C, cells were returned on ice and treated with acid wash solution (3% bovine serum albumin, 25 mM glycine, pH 2.7) to remove cell surface-bound antibody. The cells were rinsed, fixed, and processed for dual label immunofluorescence as described above. In some cases endocytosis of CTB was assessed by monitoring CTB delivery to the perinuclear region of the cell as reported previously (37, 38).

Time Lapse Microscopy—Primary keratinocytes were cultured on chambered coverglass plates (Lab-Tek/Nunc, Rochester, NY) and shifted to medium containing 0.5 mM calcium 16–18 h before treatment. Cells were then incubated with a fluorescently tagged pathogenic mouse monoclonal antibody against the extracellular domain of Dsg3, AK23 (17), to label the cell surface. Cells were then transferred to 37 °C for the indicated internalization times. An inverted Leica DMIRE2 microscope equipped with narrow band-pass filters and a Hamamatsu Electron Multiplier back-thinned and deep-cooled CCD camera (C9100-12) was used for image acquisition. Temperature control was achieved using an environmental control chamber (Pecon Incubator ML) and heated stage insert (Pecon Heating Insert P). The camera, fully motorized microscope, and automated stage were driven by Simple PCI software.

Dispase Cell Dissociation Assay—A dispase dissociation assay was performed as described previously (19). Briefly, NHK cultures were seeded in triplicate onto 35-mm dishes containing keratinocyte growth medium and allowed to grow to confluence. 24 h after reaching confluence, cultures were switched to media containing 0.5 mM calcium for 16–18 h. The cells were then pretreated with 40 mM genistein for 1 h at 37 °C (Sigma) and treated with either normal human IgG or PV IgG (diluted media containing 0.5 mM calcium) and incubated on ice for 30

min to 1 h. After incubation, cells were incubated in 1 unit/ml dispase (diluted in PBS⁺) (Roche Diagnostics) for more than 30 min. Released monolayers were subjected to mechanical stress by transferring the cell sheets to 15-ml conical tubes. The tubes were then subjected to 50 inversion cycles on a rocker panel. Fragments were counted using a dissecting microscope.

RESULTS

The mechanism by which membrane receptors are internalized can be delineated by selectively inhibiting endocytic pathways using well established procedures. These approaches include manipulating the cellular ionic environment (39, 40), altering membrane cholesterol availability (41–43), expressing dominant negative mutants, and inhibiting tyrosine kinase activity (44, 45) (Table 1). In the current study we utilized this matrix of approaches to define the mechanism of Dsg3 endocytosis and to examine the functional relationships between Dsg3 internalization and the loss of adhesion in response to pathogenic PV IgG.

PV IgG-induced Dsg3 Internalization Is Mediated by a Clathrin-independent Pathway—PV IgG binding causes Dsg3 internalization, dramatically accelerated degradation of Dsg3, and the loss of cell-cell adhesion strength (19). To determine whether PV IgG-induced Dsg3 internalization is mediated through a clathrin-dependent pathway, hypertonic sucrose and K⁺ depletion were employed to inhibit clathrin-mediated endocytosis. For these experiments, keratinocytes were incubated with either EGF (as a control) or a pathogenic antibody directed against Dsg3 (monoclonal antibody AK23) and placed at 37 °C to allow for internalization. A low pH wash was then used to remove cell surface-bound ligand without removing internalized ligands. At 37 °C, both AK23-Dsg3 and EGF-EGFR were internalized, as expected (Fig. 1, A, B, and G). K⁺ depletion and hypertonic sucrose dramatically inhibited EGF internalization, a ligand internalized via a clathrin-mediated pathway (Fig. 1, D, F, and G). In contrast, substantial Dsg3 endocytosis was still observed when clathrin-mediated endocytosis was blocked (Fig. 1, C, E, and G). These initial results suggest that Dsg3 internalization is mediated through a clathrin-independent pathway.

To further elucidate the mechanism of Dsg3 internalization, the localization of the PV-IgG-Dsg3 complex was compared with the distribution of clathrin and caveolin-1. As shown in Fig. 2, we were unable to demonstrate colocalization between Dsg3 and clathrin (A–C). However, the PV IgG-Dsg3 complex colocalized with caveolin-1 at the cell surface and in intracellular vesicular pools (Fig. 2, D–F). To determine whether the PV

Mechanism of Pemphigus Vulgaris IgG-induced Dsg3 Endocytosis

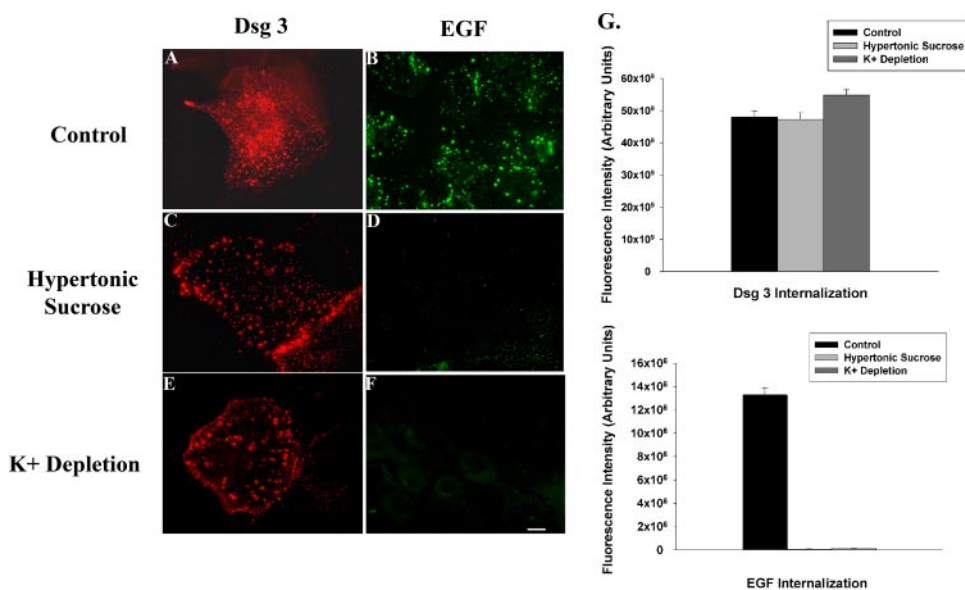


FIGURE 1. PV IgG-induced Dsg3 internalization is mediated through a clathrin-independent mechanism. Primary keratinocytes were either untreated, pretreated with hypertonic sucrose, or subjected to K^+ depletion at 37 °C. Cells were then transferred to 4 °C and incubated with either Alexa 555-labeled AK23 directed against Dsg3 (A, C, and E) or fluorescently tagged EGF (B, D, and F). Excess ligand was removed, and keratinocytes were shifted to 37 °C for 2 h to allow internalization. A low pH wash was used to remove cell surface-bound ligands to visualize internalized EGF or Dsg3. Total intracellular fluorescence was quantified using a digital imaging system and Simple PCI software (G). Error bars represent S.E., where $n = 15$ fields of view. Bar, 30 μm .

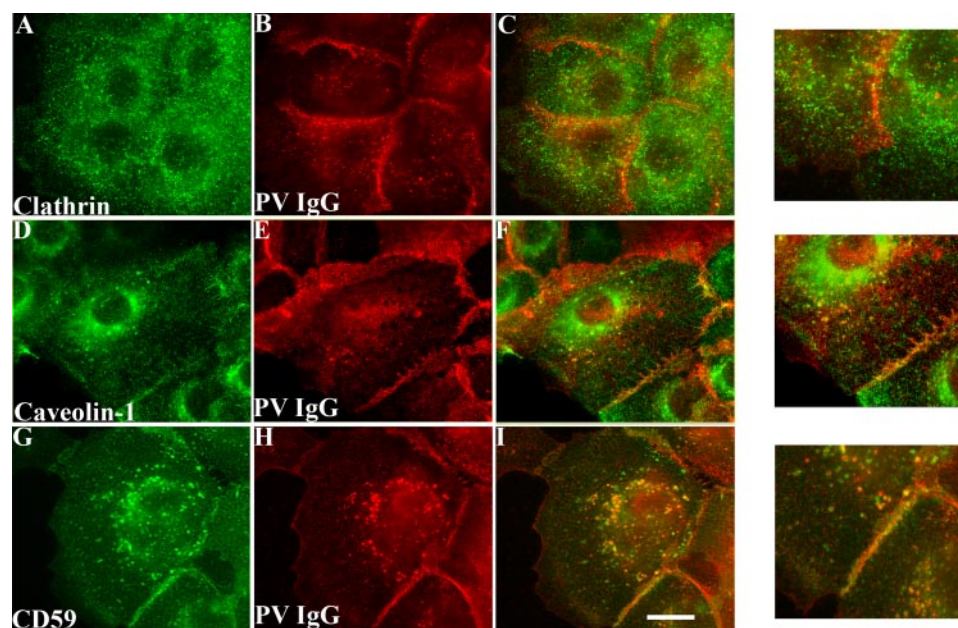


FIGURE 2. Internalized Dsg3 colocalizes with caveolin-1 and CD59 but not clathrin. Primary human keratinocytes were incubated with PV IgG for 1 h at 37 °C, fixed, and stained to observe localization of PV IgG with respect to either clathrin (A–C) or caveolin-1 (D–F) (markers of clathrin-dependent and clathrin-independent pathways, respectively). PV IgG colocalizes with caveolin-1 at both the cell surface and in intracellular vesicles, whereas PV IgG and clathrin do not colocalize. To determine whether Dsg3 internalization is mediated through lipid rafts, primary keratinocytes were incubated with both AK23 and a fluorescein isothiocyanate-labeled antibody directed against CD59 (a marker of lipid-raft dependent endocytosis) to monitor internalization of Dsg3 and CD59 after 1 h at 37 °C (G–I). Notice the extensive colocalization between the two proteins at both cell borders and in the intracellular vesicles. Bar, 10 μm .

IgG-Dsg3 complex is internalized through the use of lipid rafts, co-internalization assays were performed to monitor Dsg3 and CD59, a glycosylphosphatidyl inositol-anchored protein known to be internalized through a lipid raft-dependent pathway (46–49). Dsg3 and CD59 colocalized extensively at both

the cell surface and in vesicular pools (Fig. 2, G–I). These results further suggest that Dsg3 is internalized through a clathrin-independent mechanism.

The Cytoplasmic Tail of Dsg3 Specifies the Mechanism of Internalization—Although the extracellular domain of Dsg3 is the target of PV IgG binding, the cytoplasmic portion contains a number of domains which may play a role in mediating Dsg3 internalization. In previous studies we found that the VE-cadherin cytoplasmic tail mediates clathrin-dependent endocytosis in microvascular endothelial cells (50). These findings raise the possibility that different cell types internalize cadherins through different mechanisms or, alternatively, that different cadherins harbor determinants within their domain structure that dictate the mode of endocytosis. To distinguish these possibilities, the VE-cadherin and Dsg3 cytoplasmic tails were fused to the extracellular domain of the IL-2 receptor (IL-2R-VE-cad_{cyto} and IL-2R-Dsg3_{cyto}, respectively). These chimeric proteins were then expressed in keratinocytes for use in internalization assays in the presence or absence of agents that selectively inhibit clathrin-mediated endocytosis. As previously reported (50), internalization of the IL-2R-VE-cad_{cyto} chimera is completely eliminated upon inhibition of clathrin-dependent endocytosis (Fig. 3, D–G). However, similar to endogenous Dsg3, the IL-2R-Dsg3_{cyto} was largely refractory to inhibitors of clathrin-dependent internalization, including chlorpromazine and K^+ depletion (Fig. 3, A–C and G). These findings demonstrate that the Dsg3 cytoplasmic tail exhibits specificity for a clathrin-independent pathway.

Dsg3 Internalization Is Sensitive to Cholesterol-perturbing Agents—Cholesterol is an important component of clathrin-independent endocytosis, and numerous studies have demonstrated that cholesterol binding agents block internalization through clathrin-independent endocytic pathways (46, 51–54). Therefore, keratinocytes were pretreated with the cholesterol binding agents filipin and nystatin to determine their effects on Dsg3

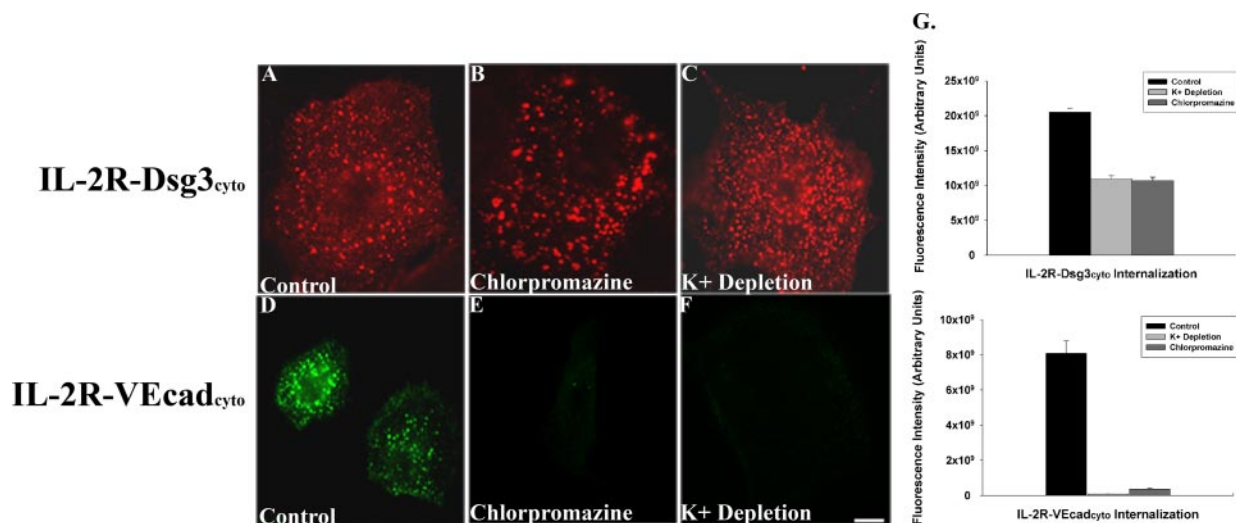


FIGURE 3. The Dsg3 cytoplasmic tail exhibits specificity for clathrin-independent internalization. Primary keratinocytes were infected with adenoviruses carrying the extracellular domain of IL-2R fused to either the Dsg3 cytoplasmic domain (*IL-2R-Dsg3_{cyto}*, A–C) or VE-cadherin cytoplasmic domain (*IL-2R-VEcad_{cyto}*, D–F). Eighteen hours after infection, keratinocytes were treated with either chlorpromazine or K⁺ depletion for 1 h at 37 °C. Cells were then transferred to 4 °C and incubated with an antibody against IL-2R. Excess ligand was removed, and keratinocytes were shifted to 37 °C for 30 min to allow internalization. A low pH media was used to remove cell surface-bound antibodies to visualize the internalized chimera. Total fluorescence was quantified using a digital imaging system and Simple PCI software (G). Error bars represent the S.E., where $n = 15$ fields of view. Bar, 30 μ m.

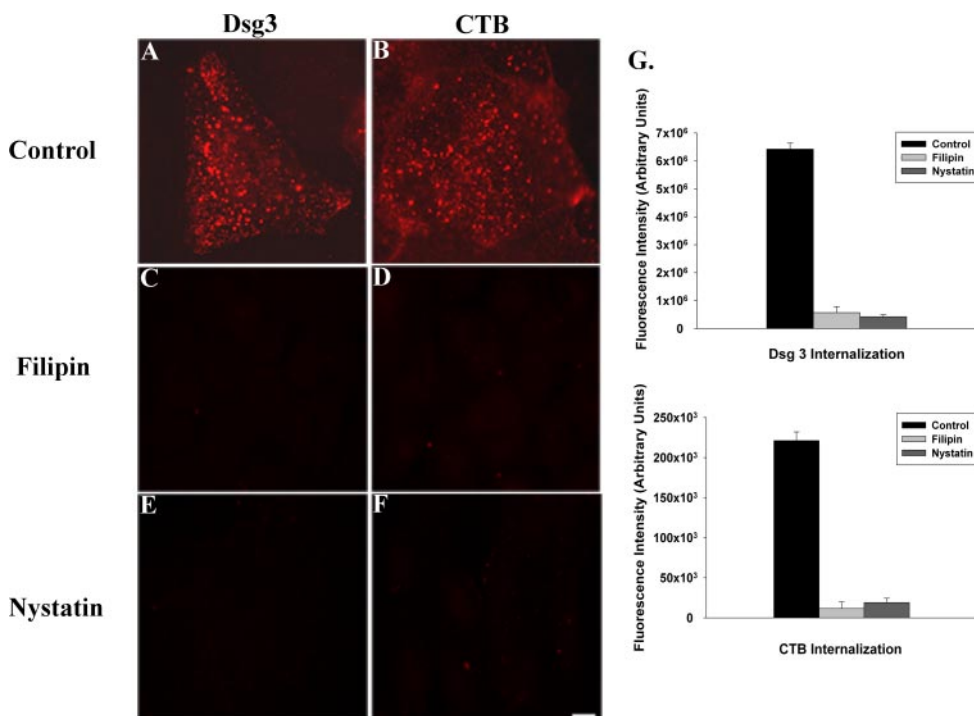


FIGURE 4. PV IgG-induced Dsg3 internalization is sensitive to cholesterol binding agents. Primary keratinocytes were either untreated or pretreated with 5 μ M filipin or 10 μ M nystatin for 1 h at 37 °C. Cells were then transferred to 4 °C and incubated with either Alexa 555-labeled AK23 directed against Dsg3 (A, C, and E) or fluorescently CTB (B, D, and F), which is known to be internalized in a clathrin-independent manner. Excess ligand was removed, and keratinocytes were shifted to 37 °C for 2 h to allow internalization. A low pH wash was used to remove cell surface-bound ligands to visualize internalized CTB or Dsg3. Total intracellular fluorescence was quantified using a digital imaging system and Simple PCI software (G). Error bars represent the S.E., where $n = 15$ fields of view. Bar, 30 μ m.

internalization. Internalization of Dsg3 was dramatically inhibited by both of these cholesterol binding agents as compared with untreated cells (Fig. 4, A, C, E, and G). Filipin and nystatin also inhibited CTB internalization, a control ligand known to be internalized via a clathrin-independent pathway (Fig. 4, B, D, F, and G).

Together, these results suggest that PV IgG internalization is mediated in a clathrin-independent and cholesterol-dependent manner.

Previous studies have demonstrated that PV IgG binding causes loss of cell surface levels of Dsg3, which correlates with an increase in Dsg3 turnover and Dsg3 internalization (19). To test whether inhibiting Dsg3 internalization stabilizes cell surface levels of Dsg3 in the presence of PV IgG, keratinocytes were either incubated with affinity-purified normal human IgG (NH IgG), PV IgG, or were pretreated with filipin before PV IgG incubation. Cell surface levels of Dsg3 were then monitored using a fluorescence-based approach as described previously (19). Keratinocytes incubated with NH IgG exhibited a slight decrease in cell surface levels of Dsg3 over a 6-h time course, representing a base-line loss of cell surface Dsg3 (Fig. 5, A, D, G, J, and M). In contrast, cell surface levels of Dsg3 in keratinocytes treated with PV IgG were dramatically reduced (Fig. 5, B, E, H, K, and M). Importantly, treating the cells with filipin prevented loss of Dsg3 cell surface levels in the presence of PV IgG (Fig. 5, C, F, I, L, and M). Similar results were observed in cells treated with NH IgG (data not shown). These results further demonstrate that cholesterol perturbation inhibits Dsg3 internalization, resulting in the retention of Dsg3 at the cell surface even in the presence of PV IgG.

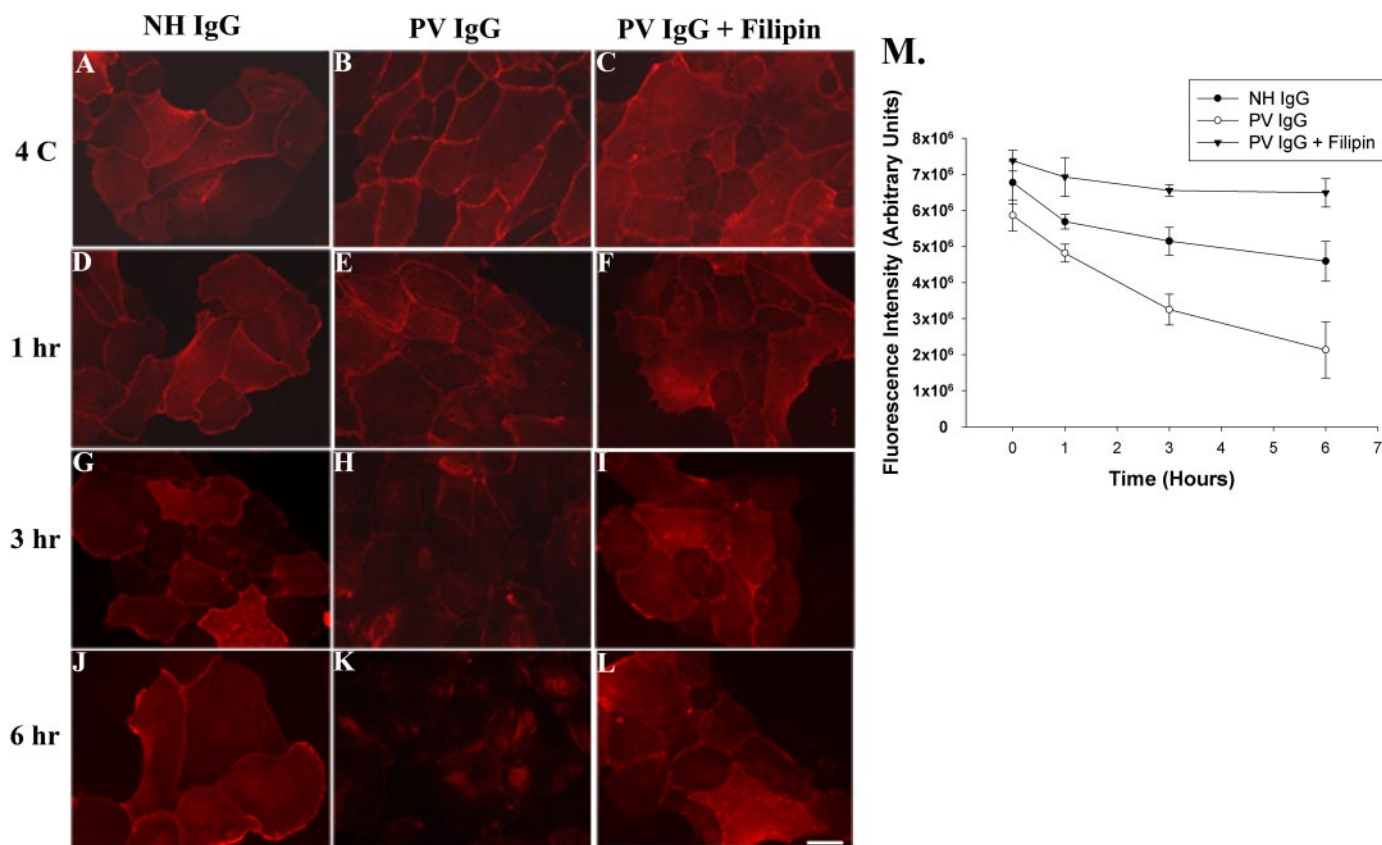


FIGURE 5. **Cholesterol perturbation prevents loss of Dsg3 cell surface levels.** Primary keratinocytes were either untreated or pretreated with 5 μ M filipin for 1 h at 37 °C. Cells were then transferred to 4 °C and incubated with either normal human IgG (A, D, G, and J) or PV IgG (B–C, E–F, H–I, and K–L). Keratinocytes were then shifted to 37 °C for various amounts of time. To measure cell surface levels of Dsg3, keratinocytes were processed for immunofluorescence analysis at each time point by fixing cells with paraformaldehyde without permeabilization. AK15, a monoclonal antibody that binds to the extracellular domain of Dsg3, was used to detect cell surface Dsg3. Total surface fluorescence was quantified using a digital imaging system and Simple PCI software (M). Error bars represent the S.E., where $n = 15$ fields of view. Bar, 40 μ m.

Dsg3 Internalization Is Dynamin- and Caveolin-independent—Clathrin-dependent and a subset of clathrin-independent endocytosis require the activity of dynamin, a GTPase responsible for pinching vesicles from the plasma membrane and thereby driving cargo internalization into carrier vesicles (33). To determine whether Dsg3 internalization is dynamin-dependent, wild type dynamin II (Dyn II WT) or a dominant negative dynamin II mutant (Dyn II K44A) was expressed in keratinocytes using an adenoviral delivery system. Expression of wild type Dyn II had no effect on either Dsg3 or EGF internalization (Fig. 6, A–C, G–I, and M). As anticipated, EGF internalization was dramatically reduced in keratinocytes expressing the dominant negative Dyn II mutant (Fig. 6, J–L and M). However, Dsg3 internalization was not affected by Dyn II K44A, indicating that Dsg3 internalization is dynamin-independent (Fig. 6, D–F and M). These results are consistent with the findings above and indicate that Dsg3 endocytosis occurs through a pathway that does not require clathrin-related mechanisms.

To further investigate the mechanisms of Dsg3 endocytosis, we examined a possible role for caveolin in Dsg3 internalization. For these experiments, a dominant negative caveolin-1 mutant (Y14F) was expressed in keratinocytes treated with PV IgG. The caveolin-1 Y14F mutant has been shown previously to disrupt caveolae and prevent caveolin-mediated endocytosis

(55, 56). To verify functional inhibition of caveolin mediated internalization, endocytosis of CTB into perinuclear compartments was monitored as described previously (37, 38). CTB internalization was dramatically inhibited in keratinocytes expressing the caveolin-1Y14F mutant (Fig. 7, A–F). In contrast, EGF endocytosis was not inhibited (Fig. 7, G–L), consistent with our findings that EGF internalization is mediated primarily through a clathrin-dependent pathway in our model system (Fig. 1). Furthermore, Dsg3 endocytosis also was unaffected by the caveolin-1 mutant (Fig. 7, M–R). Together with the results shown in Fig. 6, these findings suggest that Dsg3 endocytosis is both dynamin- and caveolin-independent.

Tyrosine Kinase Activity Is Required for PV IgG-induced Dsg3 Internalization—Clathrin-independent endocytic pathways require tyrosine kinase activity for ligand internalization (57–59). Genistein is a tyrosine kinase inhibitor shown previously to inhibit clathrin-independent internalization of a variety of ligands, including CTB (37). Therefore, keratinocytes were treated with genistein, and the internalization of Dsg3 and CTB was monitored. Extensive internalization of both Dsg3 and CTB was observed in untreated keratinocytes (Fig. 8, A, B, and E). In contrast, keratinocytes treated with genistein exhibited a dramatic reduction in both Dsg3 and CTB internalization (Fig. 8, C, D, and E).

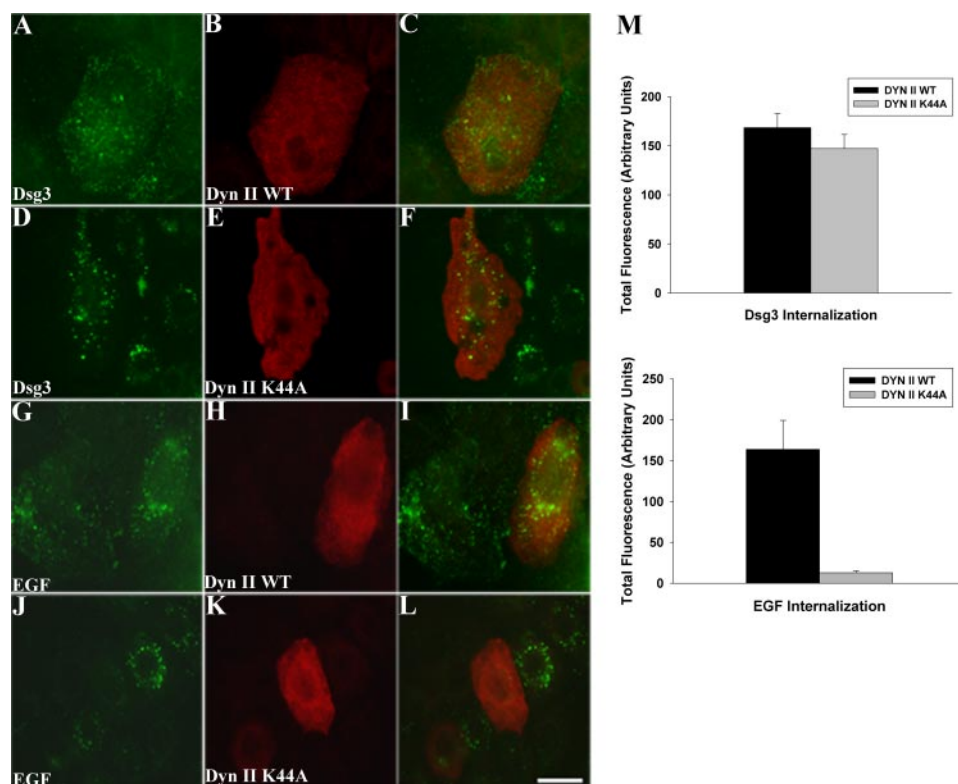


FIGURE 6. Dsg3 internalization is mediated through a dynamin-independent pathway. Primary keratinocytes were infected with adenoviruses carrying either hemagglutinin-tagged wild-type dynamin II (*Dyn II WT*) or a dominant negative mutant of dynamin II (*Dyn II K44A*). After 18 h cells were transferred to 4 °C and incubated with either an antibody against the extracellular domain of Dsg3, AK23 (A–F), or fluorescently tagged EGF (G–L). Excess ligand was removed, and keratinocytes were shifted to 37 °C for 3 h to allow internalization. Acid wash media was used to remove cell surface-bound ligands to visualize internalized EGF or Dsg3. Total fluorescence was quantified using a digital imaging system and Simple PCI software (M). Error bars represent the S.E., where $n = 20$ fields of view. Bar, 30 μm .

These results were confirmed using time lapse microscopy by following the fate of fluorescently tagged AK23 monoclonal antibody in living keratinocytes. In untreated cells, AK23 exhibited extensive redistribution from cell borders followed by internalization (Fig. 8, F–I; supplemental Movie 1). In contrast, internalization of AK23 was inhibited in genistein-treated cells (Fig. 8, J–M; supplemental Movie 2). These results indicate that in addition to cholesterol, tyrosine kinase activity also plays a role in regulating PV IgG-induced Dsg3 internalization. Both of these findings are consistent with the interpretation that Dsg3 internalization is mediated by a clathrin-independent mechanism.

Dsg3 Endocytosis Is Coupled to Depletion of Dsg3 Steady State Levels and Loss of Adhesion—Previous studies from our laboratory and others indicate that PV IgGs cause a down-regulation of Dsg3 steady state levels in cultured keratinocytes, in mouse models of disease, and in PV patient skin (19, 27, 60). To determine whether this down-regulation of Dsg3 can be prevented by agents that block Dsg3 endocytosis, keratinocytes were incubated for 24 h in the presence or absence of genistein, and Dsg3 steady state levels were monitored by Western blot analysis. As expected, PV IgG caused a down-regulation of Dsg3 in both the Triton-soluble and -insoluble pools (Fig. 9A) in untreated keratinocytes. However, genistein treatment prevented this loss of Dsg3. These data indicate that Dsg3 down-

regulation occurs through an endocytic pathway that is blocked by genistein pretreatment.

The observation that genistein blocked both Dsg3 endocytosis and depletion of steady state Dsg3 protein levels raised the possibility that inhibition of Dsg3 endocytosis might also prevent subsequent steps in disassembly and loss of adhesion. Therefore, the distribution of desmosomal components was monitored in keratinocytes pretreated with genistein in the presence of PV IgG. Normal human IgG (Fig. 9, B–D) and genistein treatment alone (Fig. 9, E–G) caused little or no change in Dsg3 and desmoplakin distribution. In contrast, PV IgG caused Dsg3 internalization and dramatic mislocalization of desmoplakin (Fig. 9, H–J). However, genistein treatment dramatically reduced Dsg3 internalization and prevented disruption of Dsg3 and desmoplakin localization at cell junctions (Fig. 9, K–M). Therefore, we assessed whether genistein could prevent loss of adhesion in functional assays in which mechanical stress is used to disrupt keratinocyte cell sheets incubated in suspension. In this assay the loss of keratinocyte adhe-

sion strength leads to the disruption of the cell sheet into numerous fragments (19, 61). Very few fragments were observed for keratinocytes incubated with either normal human IgG or genistein alone. However, numerous particles were observed when keratinocytes were incubated with PV IgG for 24 h (Fig. 9N). Importantly, genistein treatment prevented the loss of adhesion caused by PV IgG. Collectively, these findings support a model in which PV IgG causes Dsg3 endocytosis, which in turn leads to loss of Dsg3 steady state levels followed by disruption of desmosomal components and the loss of adhesion.

DISCUSSION

The results presented here suggest that PV IgG-induced Dsg3 internalization is mediated by a dynamin- and clathrin-independent mechanism. Furthermore, the Dsg3 cytoplasmic tail confers specificity for this unusual internalization pathway. Last, the results suggest that inhibiting Dsg3 internalization also prevents desmosome disassembly, decreased steady state levels of Dsg3, and loss of adhesion strength that are caused by PV IgG.

Previous studies demonstrated that upon PV IgG binding, Dsg3 is internalized and enters an endo-lysosomal pathway, leading to degradation and loss of Dsg3 steady state levels (19). The turnover rate of cell surface Dsg3 is dramatically increased

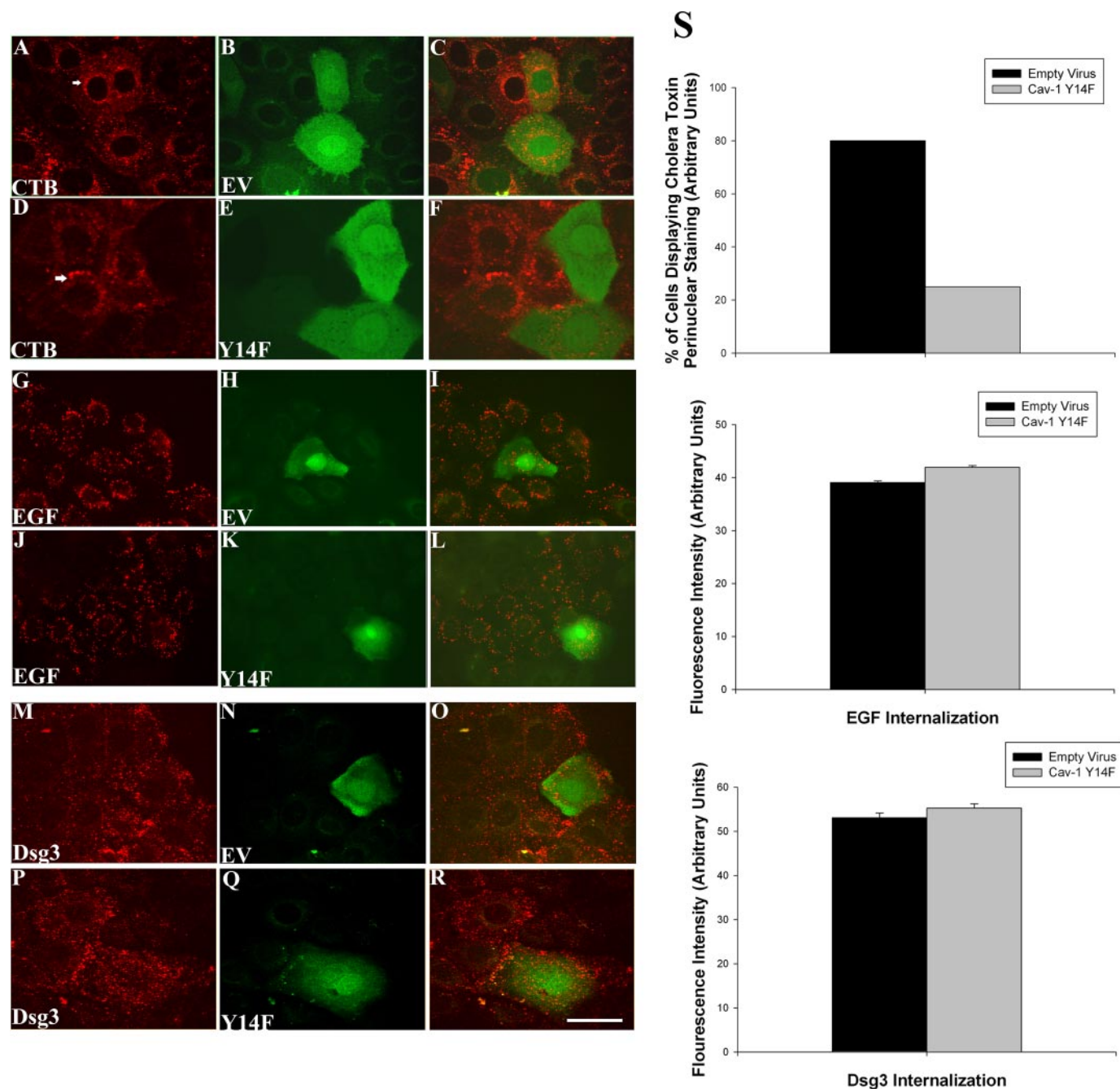


FIGURE 7. Dsg3 internalization is caveolin-independent. Primary keratinocytes were infected with adenoviruses carrying either GFP (EV) or the caveolin mutant CavY14F (Y14F). After 18 h, cells were transferred to 4 °C and incubated with either fluorescently tagged CTB (A–F), fluorescently tagged EGF (G–L), or an antibody against the extracellular domain of Dsg3, AK23 (M–R). Excess ligand was removed, and keratinocytes were shifted to 37 °C for up to 2 h to allow internalization. Acid wash media was used to remove cell surface-bound ligands to visualize internalized EGF or Dsg3. Total fluorescence was quantified using a digital imaging system and Simple PCI software (S). In the case of cholera toxin, internalization and delivery to perinuclear compartments (see the *arrow*) was used to quantify inhibition of CTB endocytosis, as reported previously (37, 38). Error bars represent the S.E., where $n = 15$ fields of view or greater. Bar, 20 μm .

in the presence of PV IgG, and this increased turnover is associated with desmosome disassembly, keratin filament retraction, and a significantly compromised ability of keratinocyte cell sheets to resist mechanical stress (19). Recently, Kitajima and co-workers (62) found that loss of Dsg3 steady state levels in cultured keratinocytes was caused specifically by Dsg3 monoclonal antibodies that are pathogenic in animal models of disease. Furthermore, studies in mouse models and analysis of human patient epidermis indicate that depletion of keratino-

cyte Dsg3 also occurs *in vivo* in response to pathogenic antibodies (63). Along with the results presented here, these findings suggest a tight coupling between Dsg3 internalization, desmosome disassembly, and the loss of adhesion during PV pathogenesis.

The data presented here suggest that Dsg3 is internalized through a lipid raft-mediated pathway upon PV IgG binding. Dsg3 internalization was dramatically inhibited by cholesterol binding agents (filipin and nystatin; Fig. 4) but largely insensi-

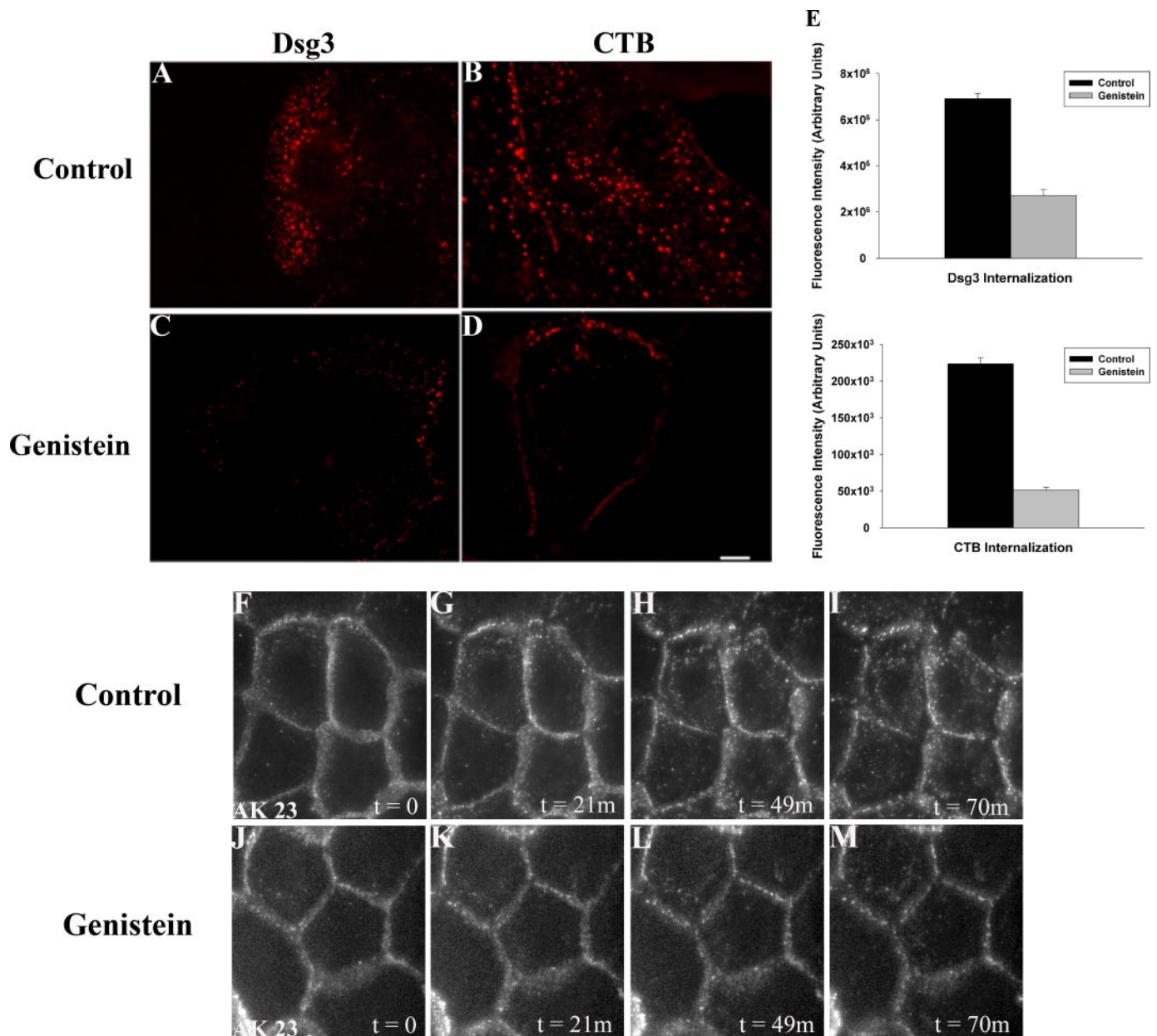


FIGURE 8. Genistein, a tyrosine kinase inhibitor, prevents PV-induced Dsg3 internalization. Primary keratinocytes were either untreated (A and B) or treated with 40 μM genistein (C and D) for 1 h at 37 °C. Cells were then transferred to 4 °C and incubated with either Alexa 555-labeled AK23 directed against Dsg3 or fluorescently tagged CTB. Excess ligand was removed, and keratinocytes were shifted to 37 °C for 2 h to allow internalization. A low pH wash was used at 4 °C to remove cell surface-bound ligands to visualize internalized cholera toxin-B or Dsg3. Total intracellular fluorescence was quantified using a digital imaging system and Simple PCI software (E). Error bars represent the S.E., where $n = 15$ fields of view. Bar, 30 μm . For time lapse experiments, living keratinocytes were incubated with fluorescently tagged AK23 at 4 °C and then transferred to 37 °C to monitor internalization of Dsg3 in either the absence (F–I) or presence of genistein (J–M). Supplemental Movies 1 and 2 correspond to panels F–I and J–M, respectively.

tive to inhibitors of clathrin-mediated pathways (Fig. 1). Furthermore, Dsg3 endocytosis was insensitive to the K44A mutant of dynamin II (60) (Fig. 6). Based on a wide range of other studies defining the characteristics of various endocytic pathways (40–45) (Table 1), this sensitivity profile suggests that Dsg3 is internalized through a lipid raft-mediated process. Consistent with this interpretation, Dsg3 co-localized extensively with the lipid raft marker CD59 at both the cell surface and in intracellular vesicular compartments (Fig. 2). Furthermore, Dsg2 was recently shown to partition into lipid rafts, raising the possibility that these detergent-insoluble membrane domains play a pertinent role in desmosome assembly and dis-

assembly (64). It is formally possible that some pools of Dsg3 are internalized by clathrin-dependent mechanisms, and partial inhibition of IL-2R-Dsg3_{cyto} chimera endocytosis was observed when the clathrin endocytic pathway was blocked (Fig. 3). One possibility is that overexpression of the IL-2R-Dsg3_{cyto} chimera causes an influx of the protein through a clathrin-mediated pathway. Alternatively, the transmembrane or extracellular domains of Dsg3 may also contain motifs responsible for conferring its specificity through a clathrin- and dynamin-independent mechanism. However, the Dsg3·PV IgG complex did not colocalize with clathrin (Fig. 2). In addition, Dsg3 internalization was dramatically inhibited by cholesterol sequestration

Mechanism of *Pemphigus Vulgaris* IgG-induced Dsg3 Endocytosis

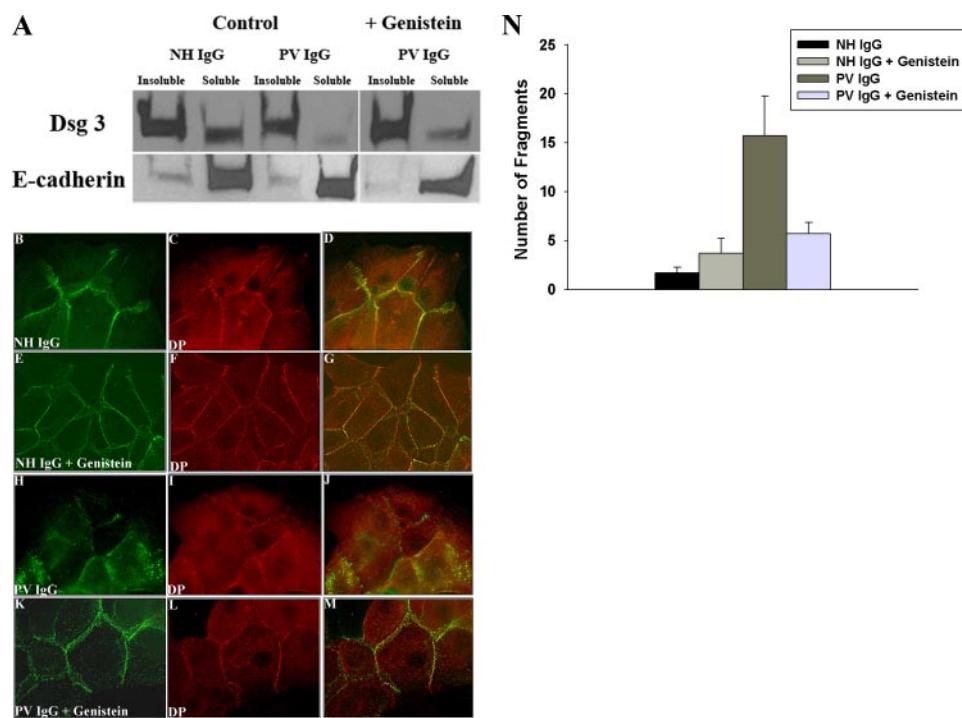


FIGURE 9. Genistein inhibits PV IgG-induced desmosomal disassembly. Steady state levels of Dsg3 were monitored via Western blot analysis. After 24 h Dsg3 levels were unchanged in the presence of normal human IgG, whereas Dsg3 levels were dramatically reduced in the presence of PV IgG. Treatment with genistein prevented this down-regulation of steady state Dsg3 levels (A). To determine the effects of genistein on displacement of desmosomal components, primary keratinocytes were either untreated (B–D and H–J) or treated with 40 μ M genistein (E–G and K–M) for 1 h at 37 °C. Cells were then transferred to 4 °C and incubated with either normal human IgG or PV IgG. Keratinocytes were then shifted to 37 °C for 4 h. Cells were fixed in cold methanol and processed for immunofluorescence to monitor Dsg3 and desmoplakin (DP) localization. To determine the effects of genistein in a functional assay, keratinocytes were grown to 100% confluency, treated for 24 h with normal human or PV IgG, and released from the substrate using dispase, an enzyme that disrupts interactions between cells and the extracellular matrix but not cell–cell adhesion. The cell sheets were placed in conical tubes and subjected to mechanical stress; the number of fragments generated directly correlates to the magnitude of the loss of cell adhesive strength. Genistein treatment dramatically reduced the number of fragments in PV IgG treated cultures (N). Bar, 30 μ m.

and the tyrosine kinase inhibitor genistein but insensitive to disruption of either dynamin or caveolin function (Figs. 6 and 7). These characteristics are hallmarks of lipid raft-mediated endocytosis (Table 1).

Cadherins have been reported to be internalized through both clathrin-dependent and -independent mechanisms depending upon the cell type. However, no detailed analysis of desmosomal cadherin endocytosis has been reported to date. In previous studies we found that VE-cadherin is internalized in a clathrin-dependent manner (50). Interestingly, IL-2R chimeras with the VE-cadherin tail appear to be internalized in both keratinocytes and endothelial cells through the same clathrin-dependent mechanism. In contrast, the IL-2R-Dsg3_{cyto} chimera is internalized in a clathrin-independent manner (Fig. 3). These results resemble the internalization profile of endogenous VE-cadherin (34) and Dsg3 under the same conditions (Figs. 1),³ demonstrating that the cytoplasmic domains of cadherins play key roles in dictating the mechanism of endocytosis independently of the cell type. The cytoplasmic tails of the Dsgs are evolutionarily divergent from the classical cad-

³ E. Delva, J. M. Jennings, C. C. Calkins, M. D. Kottke, V. Faundez, and A. P. Kowalczyk, unpublished data.

herins, such as VE-cadherin. Current studies in our laboratory are addressing which domains mediate Dsg3 endocytosis and confer specificity for clathrin-independent internalization pathways.

The results of this study support a model in which there is a functional relationship between membrane trafficking activity and desmosome disassembly in the context of PV pathophysiology. In this regard, inhibition of Dsg3 internalization and/or desmosomal disassembly may serve as potential targets for PV therapeutics. In fact, genistein was recently reported to prevent blistering in a mouse model of PV (65). Although genistein may exert effects on the desmosome independent from the regulation of Dsg3 endocytosis, these and other studies (20, 65–67) highlight the possibility that PV blistering in patients might be treated by pharmacological strategies that target keratinocyte responses to PV IgG. Likewise, Dsg3 endocytosis may be important in other aspects of keratinocyte biology. For example, desmosome assembly and desmosomal cadherin turnover may be balanced to accommodate needs for tissue integrity on the one hand and keratinocyte motility and plasticity on

the other. Understanding the mechanism involved in Dsg3 turnover and desmosomal disassembly will provide novel insight into the regulation of desmosomal dynamics during PV and perhaps other conditions where desmosomes are rapidly remodeled.

Acknowledgments—We thank members of the Kowalczyk laboratory for help and advice and Dr. Kathleen Green for helpful comments on the manuscript. We are grateful for the reagents and helpful insights provided by Drs. Masayuki Amagai, Sandra Schmid, Masuko Ushio-Fukai, Harish Radhakrishna, and Nikhil Urs.

REFERENCES

1. Yin, T., and Green, K. J. (2004) *Semin. Cell Dev. Biol.* **15**, 665–677
2. Getsios, S., Huen, A. C., and Green, K. J. (2004) *Nat. Rev. Mol. Cell Biol.* **5**, 271–281
3. Garrod, D. R., Merritt, A. J., and Nie, Z. (2002) *Curr. Opin. Cell Biol.* **14**, 537–545
4. Presland, R. B., and Dale, B. A. (2000) *Crit. Rev. Oral Biol. Med.* **11**, 383–408
5. Kottke, M. D., Delva, E., and Kowalczyk, A. P. (2006) *J. Cell Sci.* **119**, 797–806
6. Amagai, M., Klaus-Kovtun, V., and Stanley, J. R. (1991) *Cell* **67**, 869–877

7. Payne, A. S., Hanakawa, Y., Amagai, M., and Stanley, J. R. (2004) *Curr. Opin. Cell Biol.* **16**, 536–543
8. Anhalt, G. J., and Diaz, L. A. (2004) *J. Am. Acad. Dermatol.* **51**, Suppl. 1, 20–21
9. Amagai, M., Koch, P. J., Nishikawa, T., and Stanley, J. R. (1996) *J. Investig. Dermatol.* **106**, 351–355
10. Stanley, J. R., Nishikawa, T., Diaz, L. A., and Amagai, M. (2001) *J. Investig. Dermatol.* **116**, 489–490
11. Amagai, M., Hashimoto, T., Shimizu, N., and Nishikawa, T. (1994) *J. Clin. Investig.* **94**, 59–67
12. Koch, P. J., Mahoney, M. G., Ishikawa, H., Pulkkinen, L., Uitto, J., Shultz, L., Murphy, G. F., Whitaker-Menezes, D., and Stanley, J. R. (1997) *J. Cell Biol.* **137**, 1091–1102
13. Amagai, M., Ishii, K., Hashimoto, T., Gamou, S., Shimizu, N., and Nishikawa, T. (1995) *J. Investig. Dermatol.* **105**, 243–247
14. Koch, A. W., Manzur, K. L., and Shan, W. (2004) *Cell. Mol. Life Sci.* **61**, 1884–1895
15. Amagai, M., Karpati, S., Prussick, R., Klaus-Kovtun, V., and Stanley, J. R. (1992) *J. Clin. Investig.* **90**, 919–926
16. Kowalczyk, A. P., Anderson, J. E., Borgwardt, J. E., Hashimoto, T., Stanley, J. R., and Green, K. J. (1995) *J. Investig. Dermatol.* **105**, 147–152
17. Tsunoda, K., Ota, T., Aoki, M., Yamada, T., Nagai, T., Nakagawa, T., Koyasu, S., Nishikawa, T., and Amagai, M. (2003) *J. Immunol.* **170**, 2170–2178
18. Freedman, S. D., Katz, M. H., Parker, E. M., and Gelrud, A. (1999) *Am. J. Physiol.* **276**, C306–C311
19. Calkins, C. C., Setzer, S. V., Jennings, J. M., Summers, S., Tsunoda, K., Amagai, M., and Kowalczyk, A. P. (2006) *J. Biol. Chem.* **281**, 7623–7634
20. Berkowitz, P., Hu, P., Warren, S., Liu, Z., Diaz, L. A., and Rubenstein, D. S. (2006) *Proc. Natl. Acad. Sci. U. S. A.* **103**, 12855–12860
21. Waschke, J., Spindler, V., Bruggeman, P., Zillikens, D., Schmidt, G., and Drenckhahn, D. (2006) *J. Cell Biol.* **175**, 721–727
22. Williamson, L., Raess, N. A., Caldeleri, R., Zakher, A., de Bruin, A., Posthaus, H., Bolli, R., Hunziker, T., Suter, M. M., and Muller, E. J. (2006) *EMBO J.* **25**, 3298–3309
23. Sharma, P., Mao, X., and Payne, A. S. (2007) *J. Dermatol. Sci.* **48**, 1–14
24. Lanza, A., Cirillo, N., Femiano, F., and Gombos, F. (2006) *J. Cutan. Pathol.* **33**, 401–412
25. Patel, H. P., Diaz, L. A., Anhalt, G. J., Labib, R. S., and Takahashi, Y. (1984) *J. Investig. Dermatol.* **83**, 409–415
26. Iwatsuki, K., Takigawa, M., Imaizumi, S., and Yamada, M. (1989) *J. Am. Acad. Dermatol.* **20**, 578–582
27. Aoyama, Y., and Kitajima, Y. (1999) *J. Investig. Dermatol.* **112**, 67–71
28. Conner, S. D., and Schmid, S. L. (2003) *Nature* **422**, 37–44
29. Parton, R. G., and Richards, A. A. (2003) *Traffic* **4**, 724–738
30. Kirkham, M., and Parton, R. G. (2005) *Biochim. Biophys. Acta* **1745**, 273–286
31. Hill, E., van Der Kaay, J., Downes, C. P., and Smythe, E. (2001) *J. Cell Biol.* **152**, 309–323
32. Sever, S., Damke, H., and Schmid, S. L. (2000) *J. Cell Biol.* **150**, 1137–1148
33. Damke, H., Baba, T., Warnock, D. E., and Schmid, S. L. (1994) *J. Cell Biol.* **127**, 915–934
34. Xiao, K., Allison, D. F., Kottke, M. D., Summers, S., Sorescu, G. P., Faundez, V., and Kowalczyk, A. P. (2003) *J. Biol. Chem.* **278**, 19199–19208
35. LaFlamme, S. E., Thomas, L. A., Yamada, S. S., and Yamada, K. M. (1994) *J. Cell Biol.* **126**, 1287–1298
36. Setzer, S. V., Calkins, C. C., Garner, J., Summers, S., Green, K. J., and Kowalczyk, A. P. (2004) *J. Investig. Dermatol.* **123**, 426–433
37. Le, P. U., and Nabi, I. R. (2003) *J. Cell Sci.* **116**, 1059–1071
38. Yao, Q., Chen, J., Cao, H., Orth, J. D., McCaffery, J. M., Stan, R. V., and McNiven, M. A. (2005) *J. Mol. Biol.* **348**, 491–501
39. Liu, J., Kesiry, R., Periyasamy, S. M., Malhotra, D., Xie, Z., and Shapiro, J. I. (2004) *Kidney Int.* **66**, 227–241
40. Idkowiak-Baldys, J., Becker, K. P., Kitatani, K., and Hannun, Y. A. (2006) *J. Biol. Chem.* **281**, 22321–22331
41. Ros-Baro, A., Lopez-Iglesias, C., Peiro, S., Bellido, D., Palacin, M., Zorzano, A., and Camps, M. (2001) *Proc. Natl. Acad. Sci. U. S. A.* **98**, 12050–12055
42. Orlandi, P. A., and Fishman, P. H. (1998) *J. Cell Biol.* **141**, 905–915
43. Singh, R. D., Puri, V., Valiyaveetil, J. T., Marks, D. L., Bittman, R., and Pagano, R. E. (2003) *Mol. Biol. Cell* **14**, 3254–3265
44. Parton, R. G., Joggerst, B., and Simons, K. (1994) *J. Cell Biol.* **127**, 1199–1215
45. Shajahan, A. N., Timblin, B. K., Sandoval, R., Tiruppathi, C., Malik, A. B., and Minshall, R. D. (2004) *J. Biol. Chem.* **279**, 20392–20400
46. Sabharanjak, S., Sharma, P., Parton, R. G., and Mayor, S. (2002) *Dev. Cell* **2**, 411–423
47. Skretting, G., Torgersen, M. L., van Deurs, B., and Sandvig, K. (1999) *J. Cell Sci.* **112**, 3899–3909
48. Ricci, V., Galmiche, A., Doye, A., Necchi, V., Solcia, E., and Boquet, P. (2000) *Mol. Biol. Cell* **11**, 3897–3909
49. Nichols, B. J., Kenworthy, A. K., Polishchuk, R. S., Lodge, R., Roberts, T. H., Hirschberg, K., Phair, R. D., and Lippincott-Schwartz, J. (2001) *J. Cell Biol.* **153**, 529–541
50. Xiao, K., Garner, J., Buckley, K. M., Vincent, P. A., Chiasson, C. M., Dejana, E., Faundez, V., and Kowalczyk, A. P. (2005) *Mol. Biol. Cell* **16**, 5141–5151
51. Nichols, B. (2003) *J. Cell Sci.* **116**, 4707–4714
52. Lamaze, C., Dujeancourt, A., Baba, T., Lo, C. G., Benmerah, A., and Dautry-Varsat, A. (2001) *Mol. Cell* **7**, 661–671
53. Nichols, B. J., and Lippincott-Schwartz, J. (2001) *Trends Cell Biol.* **11**, 406–412
54. Puri, V., Watanabe, R., Singh, R. D., Dominguez, M., Brown, J. C., Wheatley, C. L., Marks, D. L., and Pagano, R. E. (2001) *J. Cell Biol.* **154**, 535–547
55. Orlichenko, L., Huang, B., Krueger, E., and McNiven, M. A. (2006) *J. Biol. Chem.* **281**, 4570–4579
56. Minshall, R. D., Sessa, W. C., Stan, R. V., Anderson, R. G., and Malik, A. B. (2003) *Am. J. Physiol. Lung Cell. Mol. Physiol.* **285**, 1179–1183
57. Minshall, R. D., Tiruppathi, C., Vogel, S. M., Niles, W. D., Gilchrist, A., Hamm, H. E., and Malik, A. B. (2000) *J. Cell Biol.* **150**, 1057–1070
58. Sharma, D. K., Brown, J. C., Choudhury, A., Peterson, T. E., Holicky, E., Marks, D. L., Simari, R., Parton, R. G., and Pagano, R. E. (2004) *Mol. Biol. Cell* **15**, 3114–3122
59. Damm, E. M., Pelkmans, L., Kartenbeck, J., Mezzacasa, A., Kurzchalia, T., and Helenius, A. (2005) *J. Cell Biol.* **168**, 477–488
60. Altschuler, Y., Barbas, S. M., Terlecky, L. J., Tang, K., Hardy, S., Mostov, K. E., and Schmid, S. L. (1998) *J. Cell Biol.* **143**, 1871–1881
61. Huen, A. C., Park, J. K., Godel, L. M., Chen, X., Bannon, L. J., Amargo, E. V., Hudson, T. Y., Mongiui, A. K., Leigh, I. M., Kelsell, D. P., Gumbiner, B. M., and Green, K. J. (2002) *J. Cell Biol.* **159**, 1005–1017
62. Yamamoto, Y., Aoyama, Y., Shu, E., Tsunoda, K., Amagai, M., and Kitajima, Y. (2007) *J. Biol. Chem.* **282**, 17866–17876
63. Shu, E., Yamamoto, Y., Aoyama, Y., and Kitajima, Y. (2007) *Arch. Dermatol. Res.* **299**, 165–167
64. Nava, P., Laukoetter, M. G., Hopkins, A. M., Laur, O., Gerner-Smidt, K., Green, K. J., Parkos, C. A., and Nusrat, A. (2007) *Mol. Biol. Cell* **18**, 4565–4578
65. Sanchez-Carpintero, I., Espana, A., Pelacho, B., Lopez Moratalla, N., Rubenstein, D. S., Diaz, L. A., and Lopez-Zabalza, M. J. (2004) *Br. J. Dermatol.* **151**, 565–570
66. Berkowitz, P., Diaz, L. A., Hall, R. P., and Rubenstein, D. S. (2008) *J. Investig. Dermatol.* **128**, 738–740
67. Berkowitz, P., Hu, P., Liu, Z., Diaz, L. A., Enghild, J. J., Chua, M. P., and Rubenstein, D. S. (2005) *J. Biol. Chem.* **280**, 23778–23784